JCIM JOURNAL OF CHEMICAL INFORMATION AND MODELING

pubs.acs.org/jcim Article

Molecule Edit Graph Attention Network: Modeling Chemical Reactions as Sequences of Graph Edits

Mikołaj Sacha, Mikołaj Błaż, Piotr Byrski, Paweł Dąbrowski-Tumański, Mikołaj Chromiński, Rafał Loska, Paweł Włodarczyk-Pruszyński, and Stanisław Jastrzębski*

Cite This: *J. Chem. Inf. Model.* 2021, 61, 3273−3284 Read Online

ACCESS | Metrics & More | Article Recommendations | Supporting Information

ABSTRACT: The central challenge in automated synthesis planning is to be able to generate and predict outcomes of a diverse set of chemical reactions. In particular, in many cases, the most likely synthesis pathway cannot be applied due to additional constraints, which requires proposing alternative chemical reactions. With this in mind, we present Molecule Edit Graph Attention Network (MEGAN), an end-to-end encoder−decoder neural model. MEGAN is inspired by models that express a chemical reaction as a sequence of graph edits, akin to the arrow pushing formalism. We extend this model to retrosynthesis prediction (predicting substrates given the product of a chemical reaction) and scale it up to large data sets. We argue that representing the reaction as a sequence of edits enables MEGAN to efficiently explore the space of plausible chemical reactions, maintaining the flexibility of modeling the reaction in an end-to-end fashion and achieving state-of-the-art accuracy in standard benchmarks. Code and trained models are made available online at https://github.com/molecule-one/megan.

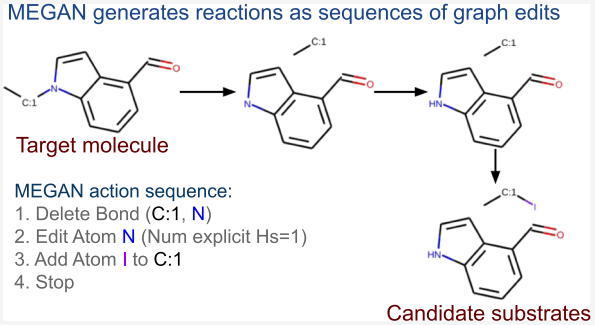

INTRODUCTION

Synthesis planning answers the question of how to make a given molecule. Due to the substantial size and complexity of the reaction space, synthesis planning is a demanding task even for skilled chemists and remains an important roadblock in the drug discovery process.[1] Computer-aided synthesis planning (CASP) methods can speed-up the drug discovery process by assisting chemists in designing syntheses.[2−5] These methods are also increasingly employed in *de novo* drug design, in which estimating the synthetic accessibility of a large number of compounds has surfaced as a key challenge to the field.[6]

Designing a synthesis plan involves predicting reaction outcomes for a given set of possible substrates (*forward synthesis prediction*) or proposing reactions that can simplify a given target molecule (*retrosynthesis prediction*).[7] In both cases, it is key for automated synthesis planning tools to model reliably outcomes of a diverse set of chemical reactions. This is especially important when there are additional constraints imposed on the desired synthesis plan such as avoiding certain starting materials or using green chemistry.[8]

A popular class of methods to predicting reaction outcomes is based on a static library of reaction templates. A reaction template encodes a graph transformation rule that can be used to generate the reaction based on the product or substrates.[2,9−16] Due to computational limitations, they typically require representing reactions using a restricted number of templates, which necessarily limits the coverage of the chemical reaction space accessible by such methods.

The small coverage and other limitations of template-based methods motivated the development of more flexible generative machine learning models, which aim to learn transformations and their applicability rules directly from the data.[17,18] Generative models have been widely used in chemistry-related tasks, including not only synthesis prediction. A variety of generative methods have been employed to design new protein structures with desired properties.[19−29] Other methods employ encoder−decoder architectures,[30,31] recurrent neural networks,[32] or reinforcement learning[33−35] to generate new drug-like molecules.

It is also worth noting that both generative or template-based approaches can be augmented by physical chemistry calculations,[36−39] which is largely complementary to our work. For instance, Guan *et al.* and[38] Ree *et al.*[39] train machine learning models on reaction data augmented with quantum mechanical descriptions.

Received: May 11, 2021
Published: July 12, 2021

Despite the added flexibility and the resulting better coverage of the chemical space, current applications of generative modeling tends to result in a limited set of plausible chemical reactions for a given input.[40] Models such as proposed in Schwaller *et al.*,[17] Karpov *et al.*,[18] Zheng *et al.*[41] belong to the class of sequence to sequence models. They generate a chemical reaction by sequentially outputting individual symbols in the SMILES notation.[42] We hypothesize this makes it challenging to generate more diverse predictions from the model, as there is no natural decomposition of the predictive distribution into plausible but different reactions. Notably, many previous papers have pointed out the limited diversity of sequence to sequence models in other domains.[43−45]

An arguably more natural idea is to express a reaction as a sequence of graph edits such as bond addition or removal, which is inspired by how chemists describe reactions using the arrow pushing mechanism.[46,47] Bradshaw *et al.*[46] introduce a model that predicts the reaction mechanism represented as a sequence of bond removal and additions that directly correspond to electron paths. However, their approach is limited to a certain subset of the chemical reaction space (reactions with linear chain topology) and forward synthesis. In a similar spirit, Do *et al.*[47] models a reaction as a set of operation on atom pairs. However, due to the lack of support for atom addition, their method also cannot be readily applied to retrosynthesis prediction. We hypothesize that expressing reaction in this way enables to easily search through different alternative reactions because the proposed reaction is obvious usually after the first few generation steps. This allows the generation algorithm to naturally backtrack and explore other possible reactions. We note that related methods have a rich history in parallel applications of generative deep learning such as natural language processing.[48]

In this work, we propose the Molecule Edit Graph Attention Network (MEGAN), an encoder−decoder end-to-end model that generates a reaction as a sequence of graph edits. Designing a novel architecture and training procedure enables us to apply this approach to both retro and forward synthesis and scale it up to large data sets. More specifically, our two main contributions are as follows:

- We extend the idea to model the reaction as a sequence edit to retrosynthesis prediction and scale it to large data sets. This required introducing a novel encoder−decoder architecture and an efficient training procedure that avoids the need to use reinforcement learning.
- We achieve competitive performance on retrosynthesis and competitive performance on forward synthesis as well as state-of-the-art top-k accuracy for large K values on all tested data sets. This serves as evidence that MEGAN achieves excellent coverage of the reaction space.

We open-sourced our code and trained models at https://github.com/molecule-one/megan.

RELATED WORK

Computer-aided reaction prediction has a rich history.[49] Early approaches to generating reactions relied on manually crafted rules,[50] which were difficult to apply to novel chemistry. Another family of methods uses physical chemistry calculations.[36] These methods are typically too computationally intensive to be used in synthesis planning software and can be complemented using statistical methods that learn from data.

Statistical approaches to predicting reactions and designing synthesis paths can be broadly categorized into template-based and template-free approaches. Template-based approaches use reaction rules or templates. These templates can be automatically mined from a database of known reactions or defined manually.[2,9−12,14,16]

Defining manually reaction templates necessitates developing complex rules governing their applicability.[14,51] This motivated the recent rise in popularity of machine-learning models used to select or rank most relevant templates.[3,52] Such models can be applied to assess the reactivity of atoms to which reaction rules should be applied.[53,54] An interesting alternative to this approach is to prioritize transformations that have already been applied to similar molecules.[55] A suitable set of templates combined with a strong ranking model can achieve state-of-the-art performance on standard retrosynthesis benchmarks.[12]

The small coverage and other limitations of template-based methods motivated the development of template-free models. A particularly successful class of template-free methods is based on sequence to sequence models that sequentially (symbol by symbol) predict the target SMILES[42] string from the input SMILES string.[42] Such approaches can be used out-of-the-box for both forward synthesis[17,56] and retrosynthesis.[18,41,57] However, they have been shown to make some trivial mistakes[51] and produce reactions with a limited diversity.[40] These models also act as black-boxes; they do not provide the reasoning behind their predictions and are not able to map atoms between the substrates and the product.

We hypothesize that the limited diversity of sequence to sequence models can be attributed to the fact that they generate reaction as a sequence of SMILES symbols from left to right. Many papers have also pointed out shortcomings in the diversity of the generated output by sequence to sequence models.[43−45] In natural language processing, there is a rich parallel history of exploring alternative generation ordering and adding through various means structure to the output. Gu *et al.*[48] show that using an alternative order of output symbols than left to right enables generating more diverse prediction. Mehri and Sigal[58] propose an alternative decoding algorithm to improve the diversity of sequence-to-sequence models that starts from generating the middle word. These modeling choices can be viewed as incorporating more suitable inductive biases for the given domain. From this perspective, we study an alternative representation of the output in generative models applied to reaction outcome prediction. Another interesting approach to increase the diversity and robustness of synthesis prediction models is to employ pretraining and augmentation methods to increase the space of reaction examples shown by the model during training.[16,59,60]

Our work focuses on a recently introduced class of template-free methods, which defines reaction generation as predicting target graph by sequentially modifying the input graph. Such an approach, while remaining template-free, can provide greater interpretability of predictions, which are modeled as direct transformations on molecules. Models that predict graph edits have been successfully applied to forward synthesis[47] and can be fine-tuned to provide especially interpretable results on certain subsets of the chemical reaction space.[46] In this work, we propose a model inspired by these prior works and extend the approach to retrosynthesis prediction.

Concurrently to our work, the graph−edit reaction generation approach has been employed to retrosynthesis in G2Gs and GraphRETRO models.[61−63] The G2Gs model presented in Shi

https://doi.org/10.1021/acs.jcim.1c00537
J. Chem. Inf. Model. 2021, 61, 3273−3284

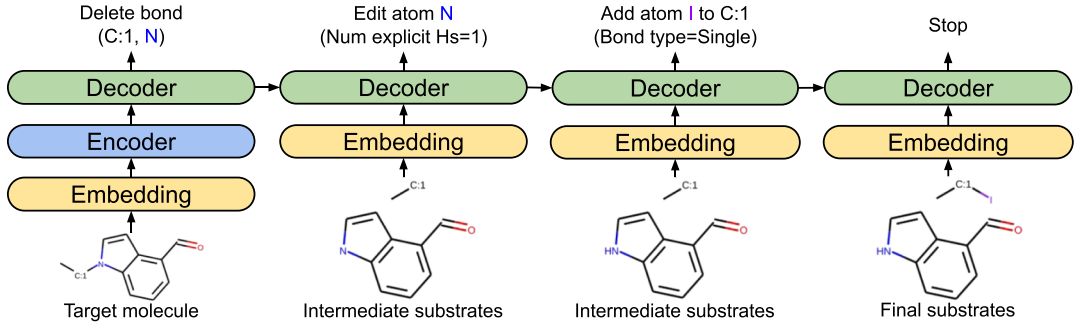

Figure 1. In the retrosynthesis prediction task, MEGAN generates substrates by sequentially modifying the target molecule. In this example, in the first step, the model decides to delete a bond between the carbon and the nitrogen atom. The generation process ends when MEGAN outputs the stop action. MEGAN is an encoder−decoder model, where the encoder and the decoder are constructed by stacking graph convolutional layers based on Graph Attention Network.[69] Before passing the graph to the encoder or decoder, we embed the atoms and bonds using one-hot encoded features, which are projected down by two separate linear layers. We describe the remaining details about the model and the used representation in Sections Input and Output Representation and Gradient-Based Training of MEGAN.

et al. and[61] Yan *et al.*[63] consists of two separate modules for predicting the reaction center and generating final substrates from the disconnected synthons. GraphRETRO[63] employs a similar framework but completes the synthons with substructures which are selected from a predefined set found on the training data. In contrast to these concurrent works, we propose an end-to-end model for generating reaction through a sequence of edits and apply it both to retro and forward synthesis prediction.

Our work on reaction outcome prediction is motivated by their wide utility. An important use of reaction outcome prediction models arises in automated synthesis planning; see, for example, Segler *et al.*[3] for an excellent discussion. It is also worth noting that reaction outcome prediction has recently risen in importance in the context of *de novo* drug discovery. Gao and Coley[6] have drawn attention to the fact that many recent *de novo* drug discovery methods tend to generate hard to synthesize molecules. In this context, automated synthesis planning can be used to filter out these hard to synthesize compounds and compares favorably to other simpler methods.[64,65] Other works use reaction outcome prediction models to define the space of accessible molecules to *de novo* models.[66] We note that our study focuses on single-step synthesis prediction; multi-step prediction has been targeted by some other works by training end-to-end models that propose whole synthesis pathways.[67,68]

Finally, a promising class of methods unifies statistical and physical calculation-based methods.[37−39] For instance, Guan *et al.* and[38] Ree *et al.*[39] train machine learning models on reaction data augmented with quantum mechanical descriptions. These methods are largely complementary to our work.

MOLECULE EDIT GRAPH ATTENTION NETWORK

MEGAN is an encoder−decoder architecture based on the graph convolutional network architecture that predicts a sequence of actions on atoms and bonds of a chemical compound.

Input and Output Representation. We begin by describing the input and the output representation of the MEGAN model.

Input representation. MEGAN takes as input a molecular graph, which is represented by labeled node vectors (atoms) and a labeled adjacency matrix (bonds).

The input $x = (\mathbf{H}^{\mathrm{OH}}, \mathbf{A}^{\mathrm{OH}})$ consists of a matrix of one-hot encoded atom features $\mathbf{H}^{\mathrm{OH}} \in \mathbb{Z}_{\geq 0}^{n \times n_a}$ and one-hot encoded bond features $\mathbf{A}^{\mathrm{OH}} \in \mathbb{Z}_{\geq 0}^{n \times n \times n_b}$, where n is the number of nodes in a graph and n_a and n_b are sizes of atom and bond feature vectors, respectively. Hydrogen atoms are removed from the graph; as for heavy atoms, the number of neighboring hydrogen atoms can be deduced implicitly.

We add an additional node to the graph named supernode,[70] which is connected to all atoms in the graph with a special supernode bond type. In graph convolutional neural networks, the supernode is particularly useful for passing information between connected components of a graph, especially after it was split by deleting a bond. Adding the supernode makes n equal to the number of atoms in the input molecule +1.

To construct feature vectors for atoms and bonds, we use the following chemical properties calculated using the RDKit package:[71] atomic number, formal charge, chiral tag, and number of explicit hydrogen atoms is aromatic for atoms and bond type and bond stereometry (none, Z or E) for bonds. All these features are set to zero for the supernode and all bonds with the supernode, except for the bond type which has a special supernode value for bonds between atoms and the supernode. We also add a binary flag to indicate whether a given atom or bond was edited or added in any of the previous steps. Finally, we indicate whether a given node is an atom or the supernode with a binary flag on each node. Final atom and bond vectors are constructed by concatenating one-hot vectors of all of their categorical features. We describe the remaining details in Supporting Information.

Output Representation. The output of MEGAN is a sequence of graph actions, which are then applied to the input graph to produce the desired output graph. An action can be applied to a single atom or a pair of atoms. In the latter case, the action modifies the bond between the two atoms. To train the model, we compare the outputted sequence of actions with the ground-truth sequence based on a mapping between the product and the substrates (see Section Gradient-Based Training of MEGAN). We define the following graph actions:

- Edit atom properties (*EditAtom*)
- Edit bond between two atoms (*EditBond*)
- Add new atom to the graph (*AddAtom*)
- Add new benzene ring to the graph (*AddBenzene*)
- Stop generation (Stop)

EditAtom changes properties of atoms, such as the formal charge, chirality, or aromaticity. *EditBond* adds, edits, or deletes a bond between two atoms. *AddAtom* adds a new atom of a

https://doi.org/10.1021/acs.jcim.1c00537
J. Chem. Inf. Model. 2021, 61, 3273−3284

specified type as a neighbor of another atom already existing in the graph, with a specified bond type. *AddBenzene* simplifies generation by allowing the model to append a complete benzene ring to a selected carbon atom. Stop action indicates the end of the generation process and can be outputted only by the supernode. To determine specific parameters, we build the vocabulary of possible actions based on the training and the validation set. We also describe in full details the possible actions on the USPTO-50k data set in Supporting Information.

Model Architecture. *Encoder−Decoder Architecture of MEGAN.* The MEGAN model consists of two parts: the encoder, which is invoked only once per reaction generation at its beginning, and the decoder, which is sequentially invoked to generate actions. This general encoder−decoder architecture is shared by the most successful sequence to sequence models in deep learning Vaswani *et al.*[72]

Both encoder and decoder are variants of graph convolutional networks (see GCN-att layer) that modify hidden vector representation of nodes. They take the same input and output node feature vector size n_a and input edge feature vector size n_b. The input graph x_t is modified according to the action predicted by the decoder at each step t, until a special Stop action is outputted. We stack n_e and n_d layers of the encoder and decoder, respectively. The architecture and the inference process are depicted schematically in Figure 1.

Generating graph actions. At each generation step t, the one-hot encoded features of the current graph $x_t = (\mathbf{H}_t^{OH}, \mathbf{A}_t^{OH})$ are first embedded using two linear layers $\mathbf{H}_t^0 = f_{emb}(\mathbf{H}_t^{OH})$ and $\mathbf{A}_t = g_{emb}(\mathbf{A}_t^{OH})$ to convert atoms and bonds to n_a and n_b-dimensional spaces, respectively. We treat n_a and n_b as hyperparameters.

In the first generation step ($t = 1$), we pass the embedded graph through the encoder and the decoder to arrive at atom features $\mathbf{H}_1 = \mathrm{dec}(\mathrm{enc}(\mathbf{H}_1^0))$. At each subsequent step t, we only use the decoder. We incorporate previous step representation by taking the element-wise maximum operation over the current and previous atom features. Namely, for $t > 1$, $\mathbf{H}_t = \mathrm{dec}(\max(\mathrm{enc}(\mathbf{H}_{t-1}), \mathbf{H}_{t-1}))$. We zero-pad features of $\mathbf{H}_{t-1}$ for any node that was added to the graph at step t. The encoder and decoder also take as input $\mathbf{A}_t$.

The logits $\mathbf{L}_t^a$ and $\mathbf{L}_t^b$ for atom actions Act_a and bond actions Act_b are calculated at each step t from $\mathbf{H}_t$ and $\mathbf{A}_t$ as follows

$$\mathbb{R}^d \ni \mathbf{F}_t = \sigma_r(g_{atom}(\mathbf{H}_t)) \tag{1}$$

$$\mathbb{R}^{|\mathrm{Act}_a|} \ni \mathbf{L}_t^a = g'_{atom}(\mathbf{F}_t) \tag{2}$$

$$\mathbb{R}^d \ni \mathbf{J}_i = \sigma_r(g_{bond}(\mathbf{H}_t)) \tag{3}$$

$$\mathbb{R}^{d+n_a} \ni \mathbf{J}'_{ij} = \sigma_r(\mathbf{J}_i + \mathbf{J}_j \| \mathbf{A}_{i,j}) \tag{4}$$

$$\mathbb{R}^{|\mathrm{Act}_b|} \ni \mathbf{L}_{tij}^b = g'_{bond}(\mathbf{J}'_{ij}) \tag{5}$$

where g_{atom}, g'_{atom}, g_{bond}, and g'_{bond} are linear layers; σ_r is the ReLU activation function. The $\|$ symbol indicates vector concatenation. To compute the final action probabilities, we apply the Softmax activation function to concatenated vectors of logits of all possible atom actions Act_a and possible bond actions Act_b.

GCN-att Layer. The basic building block of the encoder and decoder is an attention-based GCN layer that we call GCN-att. We enhance the GCN layer from Veličković *et al.*[69] by adding bond features as input information for computing the attention values. Let $\mathbf{H}_t \in \mathbb{R}^{n\times h}$ denote input node features for the t-th GCN-att layer and $N(i) \subset \mathbb{Z}_{\geq 0}$ denote set of indices of neighbors of node at index i [where $i \in N(i)$]. We calculate new node features $\mathbf{H}_{t+1} \in \mathbb{R}^{n\times h}$ as follows

$$\mathbb{R}^d \ni \mathbf{H}_i^{t'} = \sigma_r(f_{att}^{\ t}(\mathbf{H}_i^t)) \tag{6}$$

$$\mathbb{R}^{2d+n_b} \ni \mathbf{B}_{ij}^{\ t} = \mathbf{H}_i^{t'} \| \mathbf{H}_j^{t'} \| \mathbf{A}_{i,j} \tag{7}$$

$$\mathbb{R}^K \ni \mathbf{C}_{ij}^{\ t} = f_{att'}^{\ t}(\mathbf{B}_{ij}^{\ t}) \tag{8}$$

$$\mathbb{R}^{n_a} \ni \mathbf{G}_{ik}^{\ t} = \sum_{j\in N(i)} \frac{\exp \mathbf{C}_{ijk}^{\ t}}{\sum_{l\in N(i)} \exp \mathbf{C}_{ilk}^{\ t}} \mathbf{H}_j^{\ t} \tag{9}$$

$$\mathbb{R}^{n_a} \ni \mathbf{H}_i^{t+1} = \Big\|_{1\leq k\leq K} \sigma_r(f_k^{\ t}(\mathbf{G}_i^{\ t})) \tag{10}$$

where σ_r denotes ReLU activation function and $\|$ indicates vector concatenation. The scalar $K \in \mathbb{N}_+$ is the number of attention heads and $f_{att}: \mathbb{R}^{n_a} \to \mathbb{R}^d$, $f_{att'}: \mathbb{R}^{2d+n_b} \to \mathbb{R}^K$ and $f: \mathbb{R}^{n_a} \to \mathbb{R}^{n_a/K}$ are standard linear layers. Numbers n_a, n_b, d, and K are hyperparameters of the model. We require that n_a is divisible by K. We use the same hyperparameter values for all GCN-att layers in the model.

Gradient-Based Training of MEGAN. In contrast to Do *et al.*,[47] who use reinforcement learning to train their model, we back-propagate directly through the maximum likelihood objective to train MEGAN. We use teacher forcing to train the model, that is, to predict each step during reaction generation, we use previous steps from the ground-truth as input to the model.

This is nontrivial, as computing the gradient of the likelihood objective requires defining a fixed ordering of actions.[73] To solve this issue, You *et al.*[73] enumerates atoms using breadth-first search. We adapt a similar idea to reaction generation.

At first, we define a general ordering of action types for forward- and retrosynthesis. This ordering defines which types of actions should be performed first if there are more than one type of actions that could be applied to an atom in a generation step. There are various possible orderings, described in detail in the Section "Ablation Study on Action Ordering". The highest accuracy is achieved in the ordering called BFS Rand-augmented transformer (AT). In this ordering, for retrosynthesis, we give bond deletion the highest priority, as it is usually the step that determines the reaction center, which is the first step of reaction prediction in other methods.[61−63,74] Analogously, adding a bond has the highest priority for forward synthesis, as this usually determines the reaction center in forward prediction. Priorities of other types of actions were determined experimentally; we did not observe a significant change in validation error when modifying these priorities. We list these priorities explicitly in Table 1.

The remaining ties between actions are broken as follows. For retrosynthesis prediction, we prioritize actions that act on the least recently modified atoms. Our motivation is to prioritize more difficult actions (such as deciding where the reaction occurs) at the expense of simpler actions (such as completing the synthons resulting from breaking a bond). In forward prediction, we prioritize the most frequently visited atom, which we found to perform better empirically. The remaining ties are

https://doi.org/10.1021/acs.jcim.1c00537
J. Chem. Inf. Model. 2021, 61, 3273−3284

Table 1. Action Prioritization Used for Training MEGAN, for Forward and Retrosynthesis

	priorities of action types	
	retrosynthesis	forward synthesis
1	EditBond (delete)	EditBond (add)
2	EditBond (add)	EditBond (delete)
3	EditBond (other)	EditBond (other)
4	EditAtom	EditAtom
5	AddBenzene	AddBenzene
6	AddAtom	AddAtom

broken at random. We describe the algorithm in full detail in Supporting Information.

It is worth noting that the action ordering algorithm is used only to acquire ground truth samples for training MEGAN with a gradient-based method. The model is expected to learn a strong prior toward outputting edits in such order; however, when evaluating MEGAN, we do not explicitly limit the available action space, giving it a chance to determine the order by itself. We observe that MEGAN often predicts the ground truth reaction using a different order of actions than the ground truth training sample.

We use the following rules to resolve conflicts when the action could be outputted at different atoms or bonds:

- Stop action can be predicted only by the supernode
- Bond actions can be predicted for indices i and j, where $i < j$ and nodes at i and j are atoms

Finally, for simplicity, we do not mask out redundant actions, such as deleting a non-existing bond or editing the atom to the same values of properties, as we expect the model to learn not to use such actions.

EXPERIMENTS

We evaluate MEGAN on three standard data sets for retro and forward synthesis prediction. We first evaluate it on the standard retrosynthesis prediction benchmark USPTO-50k. Next, we investigate how MEGAN scales to the large-scale retrosynthesis task. Finally, we present results on forward synthesis prediction on the USPTO-MIT data set.

Retrosynthesis. *Data.* First, we evaluate MEGAN performance in retrosynthesis prediction. The goal is to predict correctly the set of reactants based on the product of a reaction. The accuracy is measured by comparing the SMILES[42] representation of the predicted molecules to the SMILES representation of the ground truth target molecules. Before the comparison, we remove atom mapping information from the SMILES strings and canonicalize them using the RDKit.[71] We use top-k accuracy computed on reactions from the test set as the main evaluation metric.

We evaluate on the USPTO-50k data set of approximately 50,000 reactions, which was collected by Lowe[75] and classified into 10 reaction types by Schneider *et al.*[76] We use the same processed version of the data set as Dai *et al.*,[12] where each reaction consists of a single product molecule and a set of one or more reactants, with corresponding atoms between the reactants and the product mapped. Following other studies, we split the reactions into training/validation/test sets with respective sizes of 80%/10%/10%. We use the data set and split provided by Dai *et al.*[12]

Experimental Setting. We run two variants of training on USPTO-50k: one with unknown reaction type and one for which reaction type is given as a prior by an additional embedding layer. For both runs, we use the same model architecture and the same training setup. The training takes approximately 16 h on a single NVIDIA Tesla K80 GPU for both variants.

We use beam search[78] on output probabilities of actions to generate multiple ranked candidates for each product. For USPTO-50k, we set the maximum number of steps to 16 and the beam width to 50, as it is the largest K for which accuracy was reported for the baseline models.

For training, we use a batch size of four reactions. We use Adam optimizer[79] with an initial learning rate of 0.0001. We use warm-up, increasing the learning rate from 0 to 0.0001 over the first 20,000 training steps. For efficiency, we evaluate the validation loss on a subset of 2500 validation samples after each 20,000 training samples. We multiply the learning rate by 0.1 if the estimated validation loss has not decreased for the last four evaluations. We stop the training after the estimated validation loss has not decreased in the last eight evaluations. We adapt the hyperparameters based on the validation loss. The final hyperparameter values are included in Supporting Information.

Baselines. We compare the performance of MEGAN on USPTO-50k with several template-free and template-based models, including current state-of-the-art methods. Seq2seq[57] and transformer[18] are both template-free methods based on machine translation models applied on SMILES strings. Retrosim[55] uses a reaction fingerprint to select a template based on similar reactions in the data set. Neuralsym[80] uses a multi-linear perceptron to rank templates. GLN[12] employs a graph model that assesses when rules from templates should be applied.

We also include a comparison to concurrently developed methods. G2G[61] is a template-free model that, similarly to MEGAN, generates reactions by modifying molecular graphs but with a separate module for predicting reaction center. GraphRETRO[63] employs two separate graph models for predicting reaction center and synthon completion. Retro-Prime[74] uses transformer-based models for both the reaction center and leaving group prediction. AT uses the transformer architecture for template-free reaction generation with some additional SMILES augmentation techniques that improve test top K accuracy but incurs additional inference cost due to the added test-time augmentation.[77] DualTB is the best performing variant of the method from Sun *et al.*[81] that uses transformer to rank reactions proposed by applying templates to the product.

Results. Table 2 reports results on the USPTO-50k benchmark in a variant with and without reaction type information provided. When the reaction type is given, MEGAN outperforms all baselines besides the concurrent DualTB model[81] in all metrics, with the exception of top-1. When the reaction type is unknown, MEGAN beats prior models for $K \geq 3$ (and concurrent models for $K \geq 10$) and achieves comparable results for lower values of K.

We hypothesize that the advantage of MEGAN for large K stems largely from the fact that MEGAN generates reaction as a sequence of edits. This might help to efficiently search through different plausible reaction centers, hence covering a more diverse subset of the reaction space. It can also enable MEGAN to achieve high coverage of the reaction space, which is indicated by the top-50 accuracy of 93.2% when the reaction type is unknown and 95.3% when the reaction type is provided.

Large-Scale Retrosynthesis Prediction Task. *Data.* The USPTO-50k benchmark, although of relatively high quality, is a

https://doi.org/10.1021/acs.jcim.1c00537
J. Chem. Inf. Model. 2021, 61, 3273−3284

Table 2. Top-k Test Accuracy for Retrosynthesis Prediction on the USPTO-50k Data set[a]

	top-k accuracy %					
methods	1	3	5	10	20	50
Reaction Type Unknown						
transformer	37.9	57.3	62.7			
retrosim	37.3	54.7	63.3	74.1	82.0	85.3
neuralsym	44.4	65.3	72.4	78.9	82.2	83.1
GLN	**52.5**	69.0	75.6	83.7	89.0	92.4
MEGAN	48.1	**70.7**	**78.4**	**86.1**	**90.3**	**93.2**
G2Gs†	48.9	67.6	72.5	75.5		
GraphRETRO†	53.7	68.3	72.2	75.5		
RetroPrime†	51.4	70.8	74.0	76.1		
AT (100x)†	53.2		**80.5**	85.2		
DualTB†	**55.2**	**74.6**	**80.5**	**86.9**		
Reaction Type Given as Prior						
seq2seq	37.4	52.4	57.0	61.7	65.9	70.7
retrosim	52.9	73.8	81.2	88.1	91.8	92.9
neuralsym	55.3	76.0	81.4	85.1	86.5	86.9
GLN	**64.2**	79.1	85.2	90.0	92.3	93.2
MEGAN	60.7	**82.0**	**87.5**	**91.6**	**93.9**	**95.3**
G2Gs†	61.0	81.3	86.0	88.7		
GraphRETRO†	63.9	81.5	85.2	88.1		
RetroPrime†	64.8	81.6	85.0	86.9		
DualTB†	**67.7**	**84.8**	**88.9**	**92.0**		

[a]MEGAN achieves state-of-the-art results for K equal, or larger than 1 compared to prior work, which demonstrates an excellent coverage of the chemical reaction space. Results of other methods are taken from Dai *et al.*,[12] Somnath *et al.*,[62] Yan *et al.*,[63] Wang *et al.*,[74] and Tetko *et al.*[77] † denotes concurrent work. We also note that AT averages predictions over 100 different augmentations, which significantly increases inference time. The best results are bolded.

small data set containing only 10 specific types of reactions. We train MEGAN for retrosynthesis on a large benchmark to test its scalability. We use the original data set collected by Lowe[75] containing reactions from US patents dating from 1976 to September 2016. We use the same preprocessed and split data as,[12] which consists of approximately 800k/100k/100k training/validation/test reactions. We refer to this data set as USPTO-FULL.

Experimental Setting. We train MEGAN on USPTO-FULL using the same architecture and training procedure as for USPTO-50k. We only increase the maximum number of actions from 16 to 32 to account for more complex reactions in the data set. We use a beam search with beam width of 50 for evaluation. Otherwise, we use the same hyperparameters as on USPTO-50k. The training took about 60 h on a single Tesla K80 GPU.

Results. Table 3 shows top-k accuracy on USPTO-FULL for MEGAN compared to other methods for retrosynthesis prediction. We see that our model achieves competitive performance on a large scale retrosynthesis data set, slightly outperforming other methods in terms of top-10 accuracy.

Forward Synthesis. *Data.* Finally, we evaluate MEGAN on forward synthesis. The goal is to predict correctly the target based on the substrates. We train the model on a standard forward synthesis benchmark of approximately 480,000 atom-mapped chemical reactions, split into training/validation/test sets of 410k/30k/40k samples, which we call USPTO-MIT.[53]

Baselines. We compare MEGAN to the following baselines. S2S[56] and MT[17] use machine translation models to predict the SMILES of the product from the SMILES of the substrates.

Table 3. Top-k Test Accuracy for Retrosynthesis Prediction on the USPTO-FULL Data set[a]

	top-k accuracy %		
methods	1	10	50
retrosim	32.8	56.1	
neuralsym	35.8	60.8	
GLN	39.3	63.7	
MEGAN	33.6	**63.9**	74.1
AT (100x)†	**44.4**	**70.4**	

[a]Results for other methods are taken from Dai *et al.*[12] and Tetko *et al.*[77] † denotes concurrent work. We also note that AT averages predictions over 100 different augmentations, which significantly increases inference time. The best results are bolded.

WLDN[53] identifies pairwise atom interactions in the reaction center and ranks enumerated feasible bond configurations between these atoms. WLDN5[54] improves this method by combining the problems of reaction center prediction and candidate ranking into a single task. GTPN[47] predicts actions on the graph of substrates, similarly to MEGAN; however, it limits them to actions between existing atom pairs. We include also the concurrent AT model[77] in the comparison.

Experimental Setting. We remove the Chiral tag and Bond stereo features from the model input, as USPTO-MIT has no stereochemical information. Forward synthesis usually takes fewer modifications to predict than retrosynthesis; so we reduce the maximum number of steps to 8 and use a beam size of 20 for evaluation. We also change the strategy to break ties in action ordering. For forward synthesis, we prioritize actions that act on most recently modified atoms. Apart from these changes, we use the same architecture, hyperparameters, and training procedure as for USPTO-50k.

Similarly to Schwaller *et al.*,[17] we train for two variants of forward synthesis prediction. For the separated variant, compounds that directly contribute to the product are explicitly marked in the set of substrates with an additional atom feature. For the mixed variant, such information is not provided, so the model has a harder task as it has to determine the reaction center from a larger number of possible reactants.

In forward synthesis, MEGAN can generate multiple products for a given set of input substrates set, whereas the USPTO-MIT set contains single−product reactions. We use a simple heuristic to acquire the main reaction product from the MEGAN prediction by selecting the product that has the longest SMILES string. From our observation, this heuristic works correctly for most of the reactions and does not lower the top K accuracies.

Results. Table 4 shows how MEGAN compares with other methods on both variants in terms of top-1 accuracy. In contrast to retrosynthesis, MEGAN is slightly outperformed by the molecular transformer[17] on both forward synthesis tasks with a test accuracy of 89.3% for separated and 86.3% for mixed. This might be attributable to the larger action space (the number of atoms and bond choices in each step) in MEGAN in the forward direction compared to the backward direction, which might hinder training. The action space is especially large on the mixed variant in which the substrates can include molecules with atoms that are not present in the target. Developing a better training strategy for forward prediction is a promising topic for future work.

In Table 5, we compare the performance of MEGAN and molecular transformer on USPTO-MIT in top K predictions. We use the best non-ensemble models provided by Schwaller *et*

https://doi.org/10.1021/acs.jcim.1c00537
J. Chem. Inf. Model. 2021, 61, 3273−3284

Table 4. Top-1 Test Accuracy for Forward Synthesis on the USPTO-MIT Data set[a]

variants	S2S	WLDN	GTPN	WLDN5	MT	AT†	MEGAN
separated	80.3	79.6	82.4	85.6	**90.4**	**91.9**	89.3
mixed		74.0			**88.6**	**90.4**	86.3

[a]Results for other methods taken from Schwaller *et al.*[17] and Tetko *et al.*[77] † denotes concurrent work.

Table 5. Top-k Test Accuracy of MEGAN and Molecular Transformer for Forward Synthesis on the USPTO-MIT Data set

	top-k accuracy %					
methods	1	2	3	5	10	20
			Separated			
MT	**90.5**	**93.7**	**94.7**	95.3	96.0	96.5
MEGAN	89.3	92.7	94.4	**95.6**	**96.7**	**97.5**
			Mixed			
MT	**88.7**	**92.1**	**93.1**	**94.2**	94.9	95.4
MEGAN	86.3	90.3	92.4	94.0	**95.4**	**96.6**

al.[17] and set the beam size to 20 during evaluation. We observe that MEGAN surpasses the accuracy of the molecular transformer for high K values, which again indicates its ability to explore the reaction space efficiently.

■ ANALYSIS AND ABLATION STUDIES

Error Analysis. To better understand model performance, we perform here an error analysis focusing on retrosynthesis prediction on the USPTO-50k data set.

We first visualize in Figure 2 MEGAN prediction on the USPTO-50k test set for random five target molecules on which the predicted substrates are different from the ground truth reaction. We observe that the first four reactions are feasible and can be executed using standard methods. The last reaction may pose difficulty because of the nontrivial regioselectivity that depends on the exact reaction conditions utilized.

To better quantify the phenomenon that the top proposed reaction is often correct despite being different from the ground truth, we sampled random 100 reactions from the USPTO-50k test set for which the predicted substrates by MEGAN differed from the ground truth substrates. We then analyzed the correctness, by labeling them into the following categories: (1) no issues detected (seen as a true chemical reaction by a chemist), (2) incorrect chirality of the substrates, (3) the reaction has a low yield and/or important side products, (4) the reaction can be executed but only in multiple stages (*e.g.*, with use of protecting groups), (5) there is a reactive functional group that participates in the reaction instead, and (6) incorrect reaction for another reason. All 200 reactions were shuffled and assigned randomly to two experienced organic chemists (Figure 3).

We show the breakdown of MEGAN errors by these categories in Figure 4 and examples of reaction in each category in Figure 4. On the whole, in 79.6% cases, the top prediction by MEGAN was deemed correct by chemists even though it differed from the ground truth prediction. In comparison, 89.5% of ground truth reactions were considered correct. Incorrect chirality of the substrates was the most common reason for reaction to be labeled as incorrect (7.1%, compared to 0.5% of ground truth reactions).

The main outcome of this error analysis is that for retrosynthesis prediction on the USPTO-50k, MEGAN

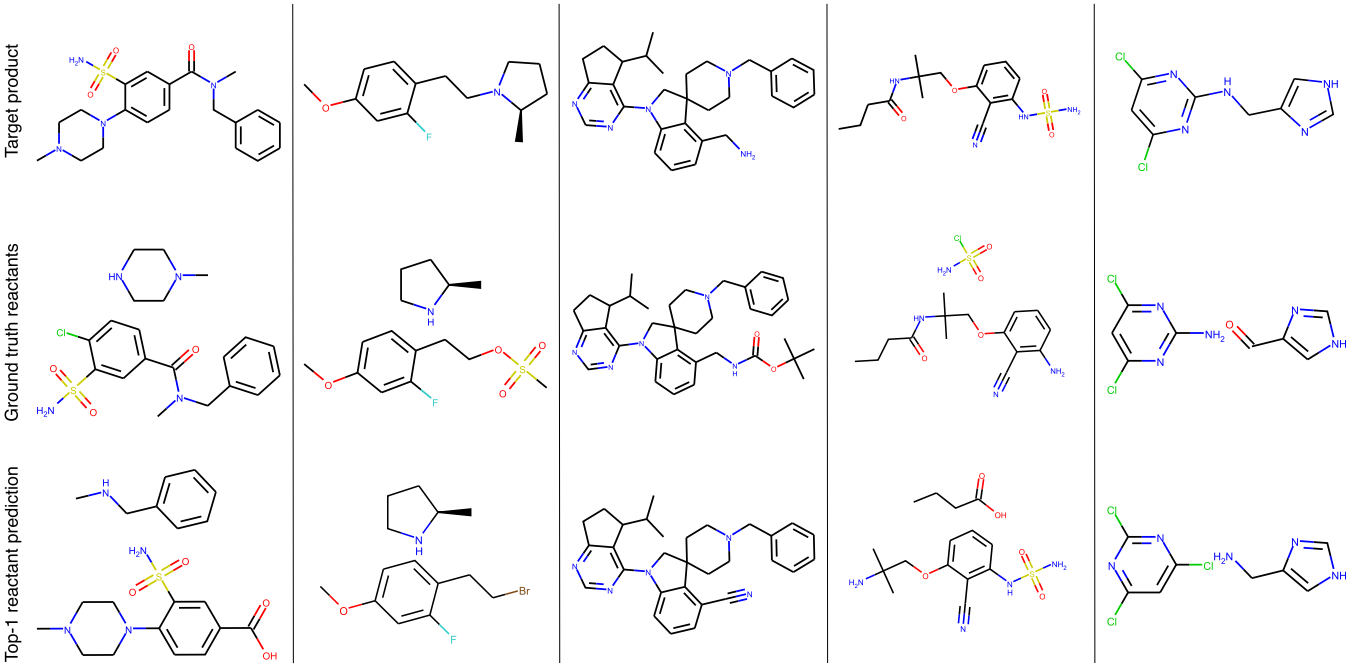

Figure 2. Top-ranked retrosynthesis prediction by MEGAN for five random target molecules from the USPTO-50k test set on which the prediction is different from the ground truth reaction. The first four reactions are feasible and can be executed using standard methods. The last reaction may pose difficulty because of the nontrivial regioselectivity that depends on the exact reaction conditions utilized.

https://doi.org/10.1021/acs.jcim.1c00537
J. Chem. Inf. Model. 2021, 61, 3273−3284

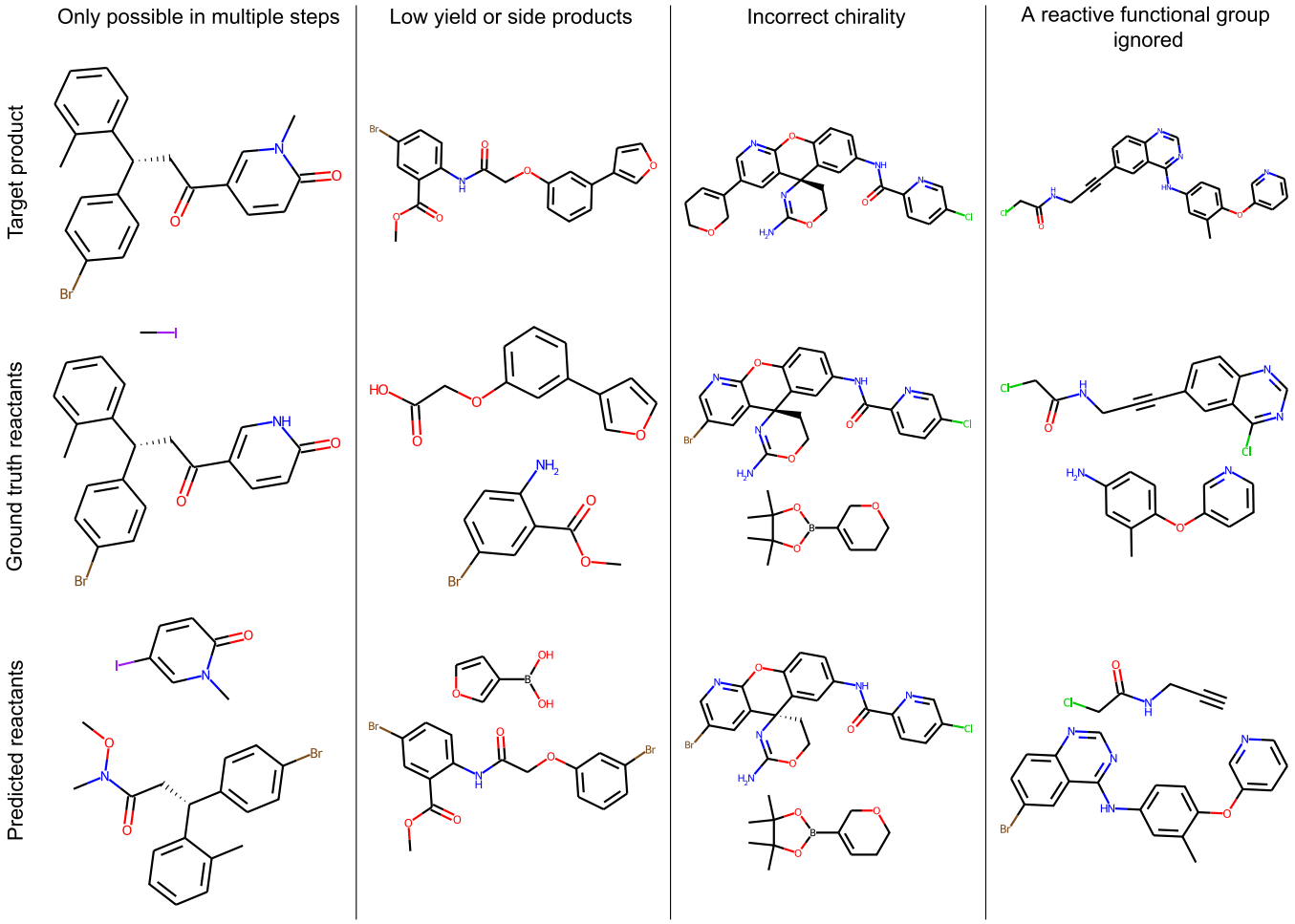

Figure 3. Examples of top-ranked retrosynthesis prediction by MEGAN for different error categories (*cf.* Figure 4).

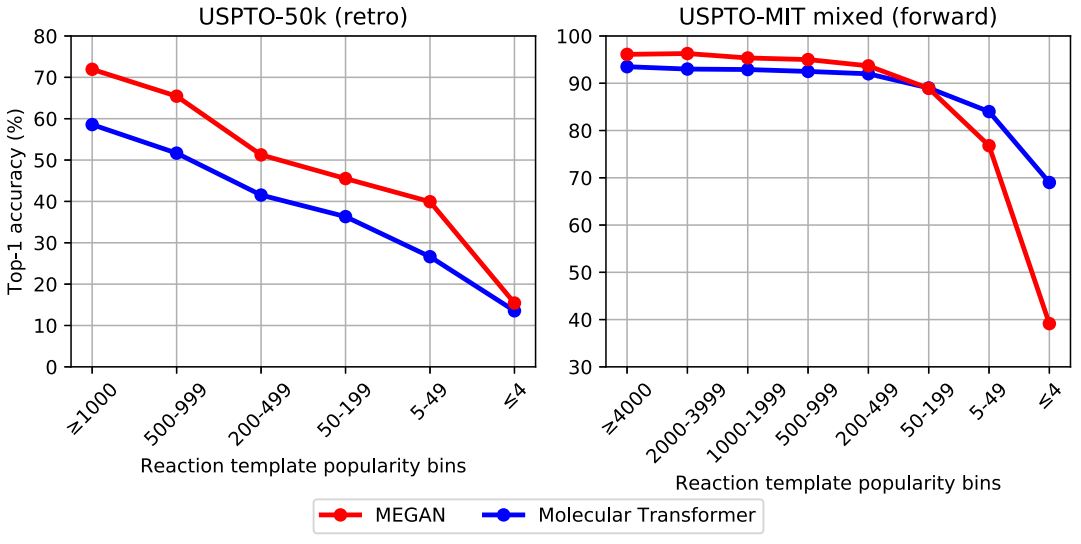

Figure 4. Top-1 test accuracy of MEGAN and molecular transformer for reactions grouped by their corresponding reaction template popularity. MEGAN achieves higher accuracy on reactions that can be described by popular reaction templates on both USPTO-50k (left) and USPTO-MIT (right).

performance seems to be close to human-level performance in the sense that the proposed reactions start to be hard to distinguish from ground-truth reactions in terms of their correctness. Having said that, there is still significant room for improvement, for example, in terms of the chirality of the proposed substrates. Another common source of errors was ignoring the existence of a reactive functional group in the substrates.

Ablation Study on Action Ordering. Our gradient-based method of training MEGAN is based on a fixed ordering on

https://doi.org/10.1021/acs.jcim.1c00537
J. Chem. Inf. Model. 2021, 61, 3273−3284

ground-truth actions. Defining this ordering requires breaking ties between different actions of the same type. For example, if there are several *EditBond* actions, we have to decide which should be executed first by the model.

In retrosynthesis prediction tasks, we broke ties based on the last time a given atom was modified. Actions that modify atoms that were least frequently modified are prioritized. The remaining ties were broken at random. We refer here to this ordering algorithm as BFS Rand-AT.

We explore here two modifications to this ordering. First, instead of prioritizing actions that modify the least frequently modified atom, we experiment with prioritizing actions that modify the most frequently modified atom. We refer to this as DFS ordering. Second, we investigate a strategy to break remaining ties based on the canonical SMILES. In this strategy, we prioritize actions that modify atoms that are earlier in the ordering determined by the canonical SMILES. We refer to this as CANO-AT. By combining these different choices, we arrive at four different ordering strategies: BFS Rand-AT, DFS Rand-AT, BFS CANO-AT, and DFS CANO-AT.

We present the performance of all variants on the USPTO-50k data set in Table 6. We observe that BFS rand-at ordering achieves the highest performance across most values of K, which motivates our choice to use it for training MEGAN on retrosynthesis prediction tasks. It is worth emphasizing that the choice of action ordering can strongly impact the performance of MEGAN. For example, the random action ordering achieves over 4% lower top-1 accuracy compared to DFS Rand-at, which we used in the experiments.

Table 6. Top-k Validation Accuracy on USPTO-50k (Reaction Type Unknown) for Different Methods of Ordering Actions on ground-truth reactions from the Train Set

	top-k accuracy %					
action order	1	3	5	10	20	50
DFS cano-at	47.6	71.2	79.5	87.0	91.4	94.2
BFS cano-at	47.5	71.8	80.2	87.0	91.4	**94.5**
DFS rand-at	43.9	67.9	76.4	83.8	88.4	92.4
BFS rand-at	**48.6**	**72.2**	**80.3**	**87.6**	**91.6**	94.2
Random	44.0	61.7	69.8	78.5	84.4	89.5

Performance with Respect to Reaction Popularity. Next, we analyze how MEGAN performance depends on reaction popularity. To approximate reaction popularity, we count the number of times that the corresponding template occurred in the training set. We use code provided by Coley *et al.*[54] to extract templates for each ground-truth reaction from the data sets.

Figure 5 compares the test accuracy of MEGAN and molecular transformer depending on the ground-truth reaction-type popularity. We use the model provided by Karpov *et al.*[18] to get transformer predictions on USPTO-50k and results from Schwaller *et al.*[17] for comparison on USPTO-MIT. We observe that MEGAN performs better on popular types of reactions and underperforms compared to molecular transformer on the rarest reactions. A natural topic for future work is to improve the performance of MEGAN on this subset of the reaction space.

CONCLUSIONS

In this work, we proposed MEGAN, a template-free model for both retrosynthesis and forward synthesis inspired by how chemists represent chemical reactions. MEGAN achieves competitive performance on both retrosynthesis and forward synthesis as well as state-of-the-art top-k accuracy for large K values on all tested data sets. MEGAN can be also scaled up to large reaction data sets.

Crucially, MEGAN generates reaction as a sequence of graph edits, which is inspired by how chemists represent chemical reactions. This inductive bias might explain the strong empirical

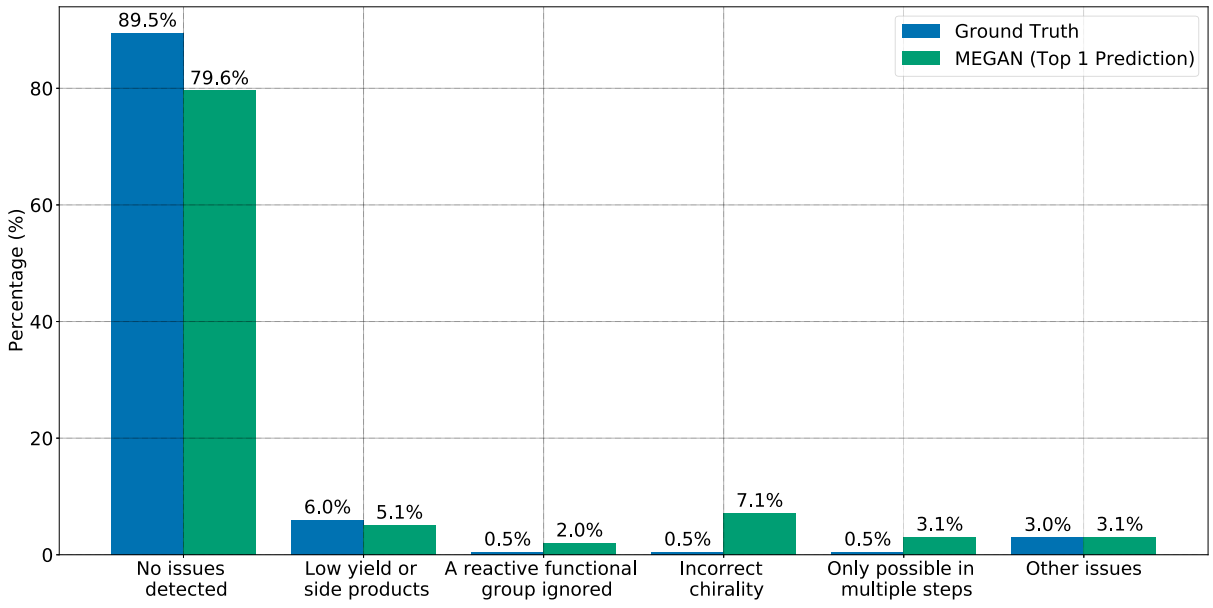

Figure 5. Categorization of the top-ranked retrosynthesis predictions by MEGAN on a subset of USPTO-50k test set on which the top prediction differs from the ground truth reaction. For reference, we also include labels assigned to ground truth reaction from the test set. We find that the top-ranked prediction is often (in 79.6% cases) deemed correct by a chemist even though it differs from the ground truth ("no issues detected"). The most common source of error is incorrectly predicting chirality in the substrates ("incorrect chirality", 7.1%).

https://doi.org/10.1021/acs.jcim.1c00537
J. Chem. Inf. Model. 2021, 61, 3273−3284

performance of the model. In particular, we argued that it enables the model to more efficiently search through the space of plausible reactions. Looking forward, generating reactions as a sequence of edits is promising for building more intuitive human−computer interaction in synthesis planning software.

A natural topic for the future is reducing the reliance of MEGAN on the mapping between products and substrates. We also found that incorrectly predicting chirality of the output was the most common source of errors on the USPTO-50k data set. Improving these aspects has the potential to further push state-of-the-art in retro and forward synthesis prediction.

In our work, we focused on predicting reaction outcomes by modeling the distribution of executed reactions. An interesting direction for the future research would be to encourage the model to output reactions that lead to molecules with desired properties, similar to some existing architectures that generate molecules[30−35]

■ ASSOCIATED CONTENT

Supporting Information

The Supporting Information is available free of charge at https://pubs.acs.org/doi/10.1021/acs.jcim.1c00537.

Detailed description of the featurization used in the MEGAN model, list of graph actions used in experiments on the USPTO-50k data set, description of the algorithm used to break ties when determining the ground truth sequence of actions in training of the MEGAN model, and values of hyperparameters used in the experiments (PDF)

■ AUTHOR INFORMATION

Corresponding Author

Stanisław Jastrzębski − *Molecule One, Warsaw 00-815, Poland;* orcid.org/0000-0003-4138-1818; Email: stan@molecule.one

Authors

Mikołaj Sacha − *Molecule One, Warsaw 00-815, Poland*

Mikołaj Błaż − *Molecule One, Warsaw 00-815, Poland*

Piotr Byrski − *Molecule One, Warsaw 00-815, Poland*

Paweł Dąbrowski-Tumański − *Molecule One, Warsaw 00-815, Poland; Faculty of Mathematics and Natural Sciences, School of Exact Sciences, Cardinal Stefan Wyszynski University, Warsaw 01-815, Poland*

Mikołaj Chromiński − *Centre of New Technologies, University of Warsaw, Warsaw 02-097, Poland*

Rafał Loska − *Institute of Organic Chemistry, Polish Academy of Sciences, Warsaw 01-224, Poland;* orcid.org/0000-0002-0823-4675

Paweł Włodarczyk-Pruszyński − *Molecule One, Warsaw 00-815, Poland*

Complete contact information is available at: https://pubs.acs.org/10.1021/acs.jcim.1c00537

Notes

The authors declare the following competing financial interest(s): Molecule.one develops software for synthesis planning which is partially based on the MEGAN model.

We open-sourced our code and trained models at https://github.com/molecule-one/megan. Our implementation is based on freely available software and is released under the MIT license. All data sets are available online, with references given in the main text.

■ REFERENCES

(1) Blakemore, D. C.; Castro, L.; Churcher, I.; Rees, D. C.; Thomas, A. W.; Wilson, D. M.; Wood, A. Organic synthesis provides opportunities to transform drug discovery. *Nat. Chem.* **2018**, *10*, 383−394.

(2) Corey, E. J.; Wipke, W. T. Computer-Assisted Design of Complex Organic Syntheses. *Science* **1969**, *166*, 178−192.

(3) Segler, M. H. S.; Preuss, M.; Waller, M. P. Planning chemical syntheses with deep neural networks and symbolic AI. *Nature* **2018**, *555*, 604−610.

(4) Coley, C. W.; Green, W. H.; Jensen, K. F. Machine Learning in Computer-Aided Synthesis Planning. *Acc. Chem. Res.* **2018**, *51*, 1281−1289 PMID: 29715002.

(5) Lee, A. A.; Yang, Q.; Sresht, V.; Bolgar, P.; Hou, X.; Klug-McLeod, J. L.; Butler, C. R. Molecular Transformer unifies reaction prediction and retrosynthesis across pharma chemical space. *Chem. Commun.* **2019**, *55*, 12152−12155.

(6) Gao, W.; Coley, C. W. The Synthesizability of Molecules Proposed by Generative Models. *J. Chem. Inf. Model.* **2020**, *60*, 5714−5723.

(7) Warren, S. *Organic Synthesis: The Disconnection Approach*; John Wiley & Sons, 2007.

(8) Struble, T. J.; et al. Current and Future Roles of Artificial Intelligence in Medicinal Chemistry Synthesis. *J. Med. Chem.* **2020**, *63*, 8667−8682.

(9) Satoh, H.; Funatsu, K. SOPHIA, a Knowledge Base-Guided Reaction Prediction System - Utilization of a Knowledge Base Derived from a Reaction Database. *J. Chem. Inf. Comput. Sci.* **1995**, *35*, 34−44.

(10) Segler, M. H. S.; Waller, M. P. Modelling Chemical Reasoning to Predict and Invent Reactions. *Chem.—Eur. J.* **2017**, *23*, 6118−6128.

(11) Coley, C. W.; Barzilay, R.; Jaakkola, T. S.; Green, W. H.; Jensen, K. F. Prediction of Organic Reaction Outcomes Using Machine Learning. *ACS Cent. Sci.* **2017**, *3*, 434−443.

(12) Dai, H.; Li, C.; Coley, C.; Dai, B.; Song, L. *Advances in Neural Information Processing Systems 32*; Wallach, H., Larochelle, H., Beygelzimer, A., d'Alché-Buc, F., Fox, E., Garnett, R., Eds., 2019; pp 8872−8882.

(13) Ishida, S.; Terayama, K.; Kojima, R.; Takasu, K.; Okuno, Y. Prediction and Interpretable Visualization of Retrosynthetic Reactions Using Graph Convolutional Networks. *J. Chem. Inf. Model.* **2019**, *59*, 5026−5033.

(14) Grzybowski, B. A.; Szymkuć, S.; Gajewska, E. P.; Molga, K.; Dittwald, P.; Wołos, A.; Klucznik, T. Chematica: A Story of Computer Code That Started to Think like a Chemist. *Chem* **2018**, *4*, 390−398.

(15) Baylon, J. L.; Cilfone, N. A.; Gulcher, J. R.; Chittenden, T. W. Enhancing Retrosynthetic Reaction Prediction with Deep Learning Using Multiscale Reaction Classification. *J. Chem. Inf. Model.* **2019**, *59*, 673−688.

(16) Fortunato, M. E.; Coley, C. W.; Barnes, B. C.; Jensen, K. F. Data augmentation and pretraining for template-based retrosynthetic prediction in computer-aided synthesis planning. *J. Chem. Inf. Model.* **2020**, *60*, 3398−3407.

(17) Schwaller, P.; Laino, T.; Gaudin, T.; Bolgar, P.; Hunter, C. A.; Bekas, C.; Lee, A. A. Molecular Transformer: A Model for Uncertainty-Calibrated Chemical Reaction Prediction. *ACS Cent. Sci.* **2019**, *5*, 1572−1583.

(18) Karpov, P.; Godin, G.; Tetko, I. V. A Transformer Model for Retrosynthesis. Artificial Neural Networks and Machine Learning. *ICANN 2019: Workshop and Special Sessions*: Cham, 2019; pp 817−830.

(19) Anand, N.; Huang, P.-S. Generative modeling for protein structures. *Proceedings of the 32nd International Conference on Neural Information Processing Systems*, 2018; pp 7505−7516.

(20) Eguchi, R. R.; Anand, N.; Choe, C. A.; Huang, P.-S. IG-VAE: Generative Modeling of Immunoglobulin Proteins by Direct 3D Coordinate Generation, 2020. https://www.bioRxiv.org/content/early/2020/08/10/2020.08.07.242347 (accessed 21 June 2021).

(21) Ingraham, J.; Garg, V.; Barzilay, R.; Jaakkola, T. Generative Models for Graph-Based Protein Design. *Advances in Neural Information Processing Systems*, Curran Associates, Inc., 2019.

(22) Anand, N.; Eguchi, R.; Huang, P. Fully differentiable full-atom protein backbone generation. *Deep Generative Models for Highly Structured Data, ICLR 2019 Workshop*: New Orleans, Louisiana, United States, 2019.
(23) Li, Z.; Nguyen, S. P.; Xu, D.; Shang, Y. Protein Loop Modeling Using Deep Generative Adversarial Network. *2017 IEEE 29th International Conference on Tools with Artificial Intelligence (ICTAI)*, 2017; pp 1085−1091.
(24) Chhibbar, P.; Joshi, A. Generating protein sequences from antibiotic resistance genes data using Generative Adversarial Networks. 2019, arXiv:1904.13240 https://arxiv.org/pdf/1904.13240.pdf (accessed June 21, 2021).
(25) Shin, J.-E.; Riesselman, A. J.; Kollasch, A. W.; McMahon, C.; Simon, E.; Sander, C.; Manglik, A.; Kruse, A. C.; Marks, D. S. Protein design and variant prediction using autoregressive generative models. *Nat. Commun.* **2021**, *12*, 2403.
(26) Han, X.; Zhang, L.; Zhou, K.; Wang, X. ProGAN: Protein solubility generative adversarial nets for data augmentation in DNN framework. *Comput. Chem. Eng.* **2019**, *131*, 106533.
(27) Repecka, D.; Jauniskis, V.; Karpus, L.; Rembeza, E.; Rokaitis, I.; Zrimec, J.; Poviloniene, S.; Laurynenas, A.; Viknander, S.; Abuajwa, W.; Savolainen, O.; Meskys, R.; Engqvist, M. K. M.; Zelezniak, A. Expanding functional protein sequence spaces using generative adversarial networks. *Nat. Mach. Intell.* **2021**, *3*, 324−333.
(28) Sabban, S.; Markovsky, M. RamaNet: Computational de novo helical protein backbone design using a long short-term memory generative neural network. *F1000Research* **2020**, *9*, 298.
(29) Karimi, M.; Zhu, S.; Cao, Y.; Shen, Y. De novo protein design for novel folds using guided conditional Wasserstein generative adversarial networks. *J. Chem. Inf. Model.* **2020**, *60*, 5667.
(30) Gao, K.; Nguyen, D. D.; Tu, M.; Wei, G.-W. Generative network complex for the automated generation of drug-like molecules. *J. Chem. Inf. Model.* **2020**, *60*, 5682.
(31) Gómez-Bombarelli, R.; Wei, J. N.; Duvenaud, D.; Hernández-Lobato, J. M.; Sánchez-Lengeling, B.; Sheberla, D.; Aguilera-Iparraguirre, J.; Hirzel, T. D.; Adams, R. P.; Aspuru-Guzik, A. Automatic chemical design using a data-driven continuous representation of molecules. *ACS Cent. Sci.* **2018**, *4*, 268−276.
(32) Segler, M. H. S.; Kogej, T.; Tyrchan, C.; Waller, M. P. Generating focused molecule libraries for drug discovery with recurrent neural networks. *ACS Cent. Sci.* **2018**, *4*, 120−131.
(33) Olivecrona, M.; Blaschke, T.; Engkvist, O.; Chen, H. Molecular de-novo design through deep reinforcement learning. *J. Cheminf.* **2017**, *9*, 48.
(34) Popova, M.; Isayev, O.; Tropsha, A. Deep reinforcement learning for de novo drug design. *Sci. Adv.* **2018**, *4*, No. eaap7885.
(35) You, J.; Liu, B.; Ying, R.; Pande, V.; Leskovec, J. Graph Convolutional Policy Network for Goal-Directed Molecular Graph Generation. *Proceedings of the 32nd International Conference on Neural Information Processing Systems*; Red Hook: NY, USA, 2018; pp 6412−6422.
(36) Zimmerman, P. M. Automated discovery of chemically reasonable elementary reaction steps. *J. Comput. Chem.* **2013**, *34*, 1385−1392.
(37) Sadowski, P.; Fooshee, D.; Subrahmanya, N.; Baldi, P. Synergies Between Quantum Mechanics and Machine Learning in Reaction Prediction. *J. Chem. Inf. Model.* **2016**, *56*, 2125−2128.
(38) Guan, Y.; Coley, C. W.; Wu, H.; Ranasinghe, D.; Heid, E.; Struble, T. J.; Pattanaik, L.; Green, W. H.; Jensen, K. F. Regio-selectivity prediction with a machine-learned reaction representation and on-the-fly quantum mechanical descriptors. *Chem. Sci.* **2021**, *12*, 2198−2208.
(39) Ree, N.; Göller, A. H.; Jensen, J. H. RegioSQM20: improved prediction of the regioselectivity of electrophilic aromatic substitutions. *J. Cheminf.* **2021**, *13*, 10.
(40) Chen, B.; Shen, T.; Jaakkola, T. S.; Barzilay, R. Learning to Make Generalizable and Diverse Predictions for Retrosynthesis. 2019, arXiv:1910.09688. https://arxiv.org/abs/1910.09688 (accessed June 17, 2021).
(41) Zheng, S.; Rao, J.; Zhang, Z.; Xu, J.; Yang, Y. Predicting retrosynthetic reactions using self-corrected transformer neural networks. *J. Chem. Inf. Model.* **2019**, *60*, 47−55.
(42) Weininger, D. SMILES, a chemical language and information system. 1. Introduction to methodology and encoding rules. *J. Chem. Inf. Comput. Sci.* **1988**, *28*, 31−36.
(43) Roberts, N.; Liang, D.; Neubig, G.; Lipton, Z. C. Decoding and Diversity in Machine Translation. 2020, arXiv:2011.13477. https://arxiv.org/abs/2011.13477 (accessed June 17, 2021).
(44) He, X.; Haffari, G.; Norouzi, M. Sequence to Sequence Mixture Model for Diverse Machine Translation. *Proceedings of the 22nd Conference on Computational Natural Language Learning*: Brussels, Belgium, 2018; pp 583−592.
(45) Jiang, S.; de Rijke, M. Why are Sequence-to-Sequence Models So Dull? Understanding the Low-Diversity Problem of Chatbots. *Proceedings of the 2018 EMNLP Workshop SCAI: The 2nd International Workshop on Search-Oriented Conversational AI*: Brussels, Belgium, 2018; pp 81−86.
(46) Bradshaw, J.; Kusner, M. J.; Paige, B.; Segler, M. H. S.; Hernández−Lobato, J. M. A Generative Model For Electron Paths. 2018, arXiv:1805.10970. https://arxiv.org/abs/1805.10970 (accessed June 17, 2021).
(47) Do, K.; Tran, T.; Venkatesh, S. Graph Transformation Policy Network for Chemical Reaction Prediction. *Proceedings of the 25th ACM SIGKDD International Conference on Knowledge Discovery & Data Mining*: New York, NY, USA, 2019; pp 750−760.
(48) Gu, J.; Liu, Q.; Cho, K. Insertion-based Decoding with Automatically Inferred Generation Order. *Trans. Assoc. Comput. Linguist.* **2019**, *7*, 661.
(49) Todd, M. H. Computer-aided organic synthesis. *Chem. Soc. Rev.* **2005**, *34*, 247−266.
(50) Salatin, T. D.; Jorgensen, W. L. Computer-assisted mechanistic evaluation of organic reactions. 1. Overview. *J. Org. Chem.* **1980**, *45*, 2043−2051.
(51) Molga, K.; Gajewska, E. P.; Szymkuć, S.; Grzybowski, B. A. The logic of translating chemical knowledge into machine-processable forms: a modern playground for physical-organic chemistry. *React. Chem. Eng.* **2019**, *4*, 1506−1521.
(52) Wei, J. N.; Duvenaud, D.; Aspuru-Guzik, A. Neural Networks for the Prediction of Organic Chemistry Reactions. *ACS Cent. Sci.* **2016**, *2*, 725−732.
(53) Jin, W.; Coley, C. W.; Barzilay, R.; Jaakkola, T. Predicting Organic Reaction Outcomes with Weisfeiler-Lehman Network. 2017, arXiv:1709.04555. https://arxiv.org/abs/1709.04555 (accessed June 17, 2021).
(54) Coley, C. W.; Jin, W.; Rogers, L.; Jamison, T. F.; S Jaakkola, T.; Green, W. H.; Barzilay, R.; Jensen, K. F. A Graph-Convolutional Neural Network Model for the Prediction of Chemical Reactivity, 2018. https://chemrxiv.org/articles/A_Graph-Convolutional_Neural_Network_Model_for_the_Prediction_of_Chemical_Reactivity/7163189/1 (accessed 17 June 2021).web
(55) Coley, C. W.; Rogers, L.; Green, W. H.; Jensen, K. F. Computer-Assisted Retrosynthesis Based on Molecular Similarity. *ACS Cent. Sci.* **2017**, *3*, 1237−1245 PMID: 29296663.
(56) Schwaller, P.; Gaudin, T.; Lányi, D.; Bekas, C.; Laino, T. "Found in Translation": predicting outcomes of complex organic chemistry reactions using neural sequence-to-sequence models. *Chem. Sci.* **2018**, *9*, 6091−6098.
(57) Liu, B.; Ramsundar, B.; Kawthekar, P.; Shi, J.; Gomes, J.; Luu Nguyen, Q.; Ho, S.; Sloane, J.; Wender, P.; Pande, V. Retrosynthetic reaction prediction using neural sequence-to-sequence models. *ACS Cent. Sci.* **2017**, *3*, 1103−1113.
(58) Mehri, S.; Sigal, L. Middle-Out Decoding. *Advances in Neural Information Processing Systems*, Curran Associates, Inc., 2018.
(59) Zhang, Y.; Wang, L.; Wang, X.; Zhang, C.; Ge, J.; Tang, J.; Su, A.; Duan, H. Data augmentation and transfer learning strategies for reaction prediction in low chemical data regimes. *Org. Chem. Front.* **2021**, *8*, 1415−1423.

(60) Pesciullesi, G.; Schwaller, P.; Laino, T.; Reymond, J.-L. Transfer learning enables the molecular transformer to predict regio-and stereoselective reactions on carbohydrates. *Nat. Commun.* **2020**, *11*, 4874.
(61) Shi, C.; Xu, M.; Guo, H.; Zhang, M.; Tang, J. A Graph to Graphs Framework for Retrosynthesis Prediction. *Proceedings of the 37th International Conference on Machine Learning*, 2020; pp 8818−8827.
(62) Somnath, V. R.; Bunne, C.; Coley, C. W.; Krause, A.; Barzilay, R. Learning Graph Models for Retrosynthesis Prediction. 2021, arXiv:2006.07038. https://arxiv.org/abs/2006.07038 (accessed June 17, 2021).
(63) Yan, C.; Ding, Q.; Zhao, P.; Zheng, S.; Yang, J.; Yu, Y.; Huang, J. RetroXpert: Decompose Retrosynthesis Prediction like A Chemist, 2020. https://chemrxiv.org/articles/preprint/Interpretable_Retrosynthesis_Prediction_in_Two_Steps/11869692/3 (accessed 17 June 2021).
(64) Liu, C.-H.; Korablyov, M.; Jastrzębski, S.; Włodarczyk-Pruszyński, P.; Bengio, Y.; Segler, M. H. RetroGNN: Approximating Retrosynthesis by Graph Neural Networks for De Novo Drug Design. 2020, arXiv:2011.13042. https://arxiv.org/abs/2011.13042 (accessed June 17, 2021).
(65) Thakkar, A.; Chadimová, V.; Bjerrum, E. J.; Engkvist, O.; Reymond, J.-L. Retrosynthetic accessibility score (RAscore) − rapid machine learned synthesizability classification from AI driven retrosynthetic planning. *Chem. Sci.* **2021**, *12*, 3339−3349.
(66) Gottipati, S. K.; Sattarov, B.; Niu, S.; Pathak, Y.; Wei, H.; Liu, S.; Liu, S.; Blackburn, S.; Thomas, K.; Coley, C.; Tang, J.; Chandar, S.; Bengio, Y. Learning to Navigate The Synthetically Accessible Chemical Space Using Reinforcement Learning. *Proceedings of the 37th International Conference on Machine Learning*, 2020; pp 3668−3679.
(67) Lin, K.; Xu, Y.; Pei, J.; Lai, L. Automatic retrosynthetic route planning using template-free models. *Chem. Sci.* **2020**, *11*, 3355−3364.
(68) Schwaller, P.; Petraglia, R.; Zullo, V.; Nair, V. H.; Haeuselmann, R. A.; Pisoni, R.; Bekas, C.; Iuliano, A.; Laino, T. Predicting retrosynthetic pathways using transformer-based models and a hyper-graph exploration strategy. *Chem. Sci.* **2020**, *11*, 3316−3325.
(69) Veličković, P.; Cucurull, G.; Casanova, A.; Romero, A.; Liò, P.; Bengio, Y. Graph Attention Networks. *International Conference on Learning Representations*, 2018.
(70) Li, J.; Cai, D.; He, X. Learning Graph-Level Representation for Drug Discovery. 2017, arXiv:1709.03741. https://arxiv.org/abs/1709.03741 (accessed June 17, 2021).
(71) Landrum, G. RDKit: Open-source cheminformatics. http://www.rdkit.org (accessed 17 June 2021).
(72) Vaswani, A.; Shazeer, N.; Parmar, N.; Uszkoreit, J.; Jones, L.; Gomez, A. N.; Kaiser, L.; Polosukhin, I. Attention Is All You Need. 2017, arxiv:1706.03762. https://arxiv.org/abs/1706.03762 (accessed June 17, 2021).
(73) You, J.; Ying, R.; Ren, X.; Hamilton, W.; Leskovec, J. GraphRNN: Generating Realistic Graphs with Deep Auto-regressive Models. *Proceedings of the 35th International Conference on Machine Learning*; Stockholmsmässan: Stockholm Sweden, 2018; pp 5708−5717.
(74) Wang, X.; Qiu, J.; Li, Y.; Chen, G.; Liu, H.; Liao, B.; Hsieh, C.-Y.; Yao, X. RetroPrime: A Chemistry-Inspired and Transformer-based Method for Retrosynthesis Predictions, 2020. https://chemrxiv.org/articles/preprint/RetroPrime_A_Chemistry-Inspired_and_Transformer-based_Method_for_Retrosynthesis_Predictions/12971942/1 (accessed 17 June 2021).
(75) Lowe, D. Extraction of chemical structures and reactions from the literature. Ph.D. Thesis; University of Cambridge, 2012.
(76) Schneider, N.; Stiefl, N.; Landrum, G. A. What's What: The (Nearly) Definitive Guide to Reaction Role Assignment. *J. Chem. Inf. Model.* **2016**, *56*, 2336−2346 PMID: 28024398.
(77) Tetko, I. V.; Karpov, P.; Van Deursen, R.; Godin, G. State-of-the-art augmented NLP transformer models for direct and single-step retrosynthesis. *Nat. Commun.* **2020**, *11*, 5575.
(78) Graves, A. Sequence Transduction with Recurrent Neural Networks. 2012, arXiv:1211.3711. https://arxiv.org/abs/1211.3711 (accessed June 17, 2021).
(79) Kingma, D. P.; Ba, J. Adam: A Method for Stochastic Optimization. 2014, arXiv:1412.6980. http://arxiv.org/abs/1412.6980 (accessed June 17, 2021). Published as a conference paper at the 3rd International Conference for Learning Representations, San Diego, 2015.
(80) Segler, M. H. S.; Waller, M. P. Neural-Symbolic Machine Learning for Retrosynthesis and Reaction Prediction. *Chem.—Eur. J.* **2017**, *23*, 5966−5971.
(81) Sun, R.; Dai, H.; Li, L.; Kearnes, S.; Dai, B. Energy-based View of Retrosynthesis. 2020, arXiv:2007.13437. https://arxiv.org/abs/2007.13437 (accessed June 21, 2021).

https://doi.org/10.1021/acs.jcim.1c00537
J. Chem. Inf. Model. 2021, 61, 3273−3284